Approximate Probabilistic Inference for Time-Series Data: A Robust Latent Gaussian Model with Temporal Awareness

Anton Johansson[a] and Arunselvan Ramaswamy*[b]
Department of Mathematics and Computer Science, Karlstad University, Universitetsgatan 2, 65188 Karlstad, Sweden
{*anton.johansson, arunselvan.ramaswamy*}*@kau.se*

Keywords: Recurrent Neural Network (RNN), Approximative Inference, Deep Latent Gaussian Model (DLGM), Time-Series Data, Variational Recurrent Neural Network (VRNN), Generative AI.

Abstract: The development of robust generative models for highly varied non-stationary time-series data is a complex and important problem. Traditional models for time-series data prediction, such as Long Short-Term Memory (LSTM), are inefficient and generalize poorly as they cannot capture complex temporal relationships. In this paper, we present a probabilistic generative model that can be trained to capture complex temporal information, and that is robust to data errors. We call it Time Deep Latent Gaussian Model (tDLGM). Its novel architecture is an extension of the popular Deep Latent Gaussian Model (DLGM). Our model is trained to minimize a novel regularized version of the free energy loss function (an upper bound for the negative log loss). Our regularizer, which accounts for data trends, facilitates robustness to data errors that arise from additive noise. Experiments conducted show that tDLGM is able to reconstruct and generate complex time-series data. Further, the prediction error does not increase in the presence of additive Gaussian noise.

1 INTRODUCTION

Time-series prediction constitutes an important class of problems in the field of machine learning. It finds applications in numerous areas, such as traffic and demand prediction in the fifth generation of communication networks (5G), weather forecasting, traffic prediction in vehicular networks, etc. In such scenarios, the arising time-series data is highly varied and noisy, and the associated data distributions are non-stationary (time-dependent). Additionally, collecting this data is often expensive and time-consuming. One important example is in the field of wireless communication, e.g., 5G, where researchers collect customer usage patterns and traffic, and performance of service providers, over time. Such data, in addition to being expensive is often not publicly available (Mehmeti and Porta, 2021). Another scenario with the aforementioned characteristics is the field of self-driving cars (Yin and Berger, 2017). Both the 5G and self-driving car scenarios contain highly varied time-series data and, as such, exhibit complex temporal patterns. The traffic load in a 5G network is highly dependent on the time of day. Likewise, the traffic behavior in a vehicular network varies based on region, type of road, time of day, etc. There is a need to develop robust, probabilistic models for time-series data prediction. Such models can be used for robust planning, augmenting limited datasets (robust synthetic data generation), value imputation to overcome noise, training AI agents in a robust manner, etc.Robustness is an important property since the available data is often noisy. In this paper, we are interested in probabilistic models since they are expected to generalize better.

Recurrent Neural Network (RNN) is a simple and popular model for time-series data prediction. It varies from regular feed-forward networks through the use of specialized time-aware neurons. Long Short-Term Memory (LSTM) and Gated Recurrent Unit (GRU) are two important choices for neurons when building RNNs (Hochreiter and Schmidhuber, 1997; Chung et al., 2014). Our model, Time Deep Latent Gaussian Model (tDLGM), is built using LSTM units. Every LSTM unit has a cell state. A cell state is a value that aims to capture short-term as well as long-term temporal information passing through that unit. Let $\mathbf{s}$ represent the vector of all the LSTM cell states from an RNN, and let x be the input to the RNN. Passing x through the said RNN changes the cell states of all the constituent LSTM units to

[a] https://orcid.org/0009-0000-9725-1890
[b] https://orcid.org/0000-0001-7547-8111
*Ramaswamy was partially supported by The Knowledge Foundation (grant no. 20200164)

Johansson, A. and Ramaswamy, A.
Approximate Probabilistic Inference for Time-Series Data: A Robust Latent Gaussian Model with Temporal Awareness.
DOI: 10.5220/0013154800003890

In *Proceedings of the 17th International Conference on Agents and Artificial Intelligence (ICAART 2025) - Volume 2*, pages 310-321
ISBN: 978-989-758-737-5; ISSN: 2184-433X

$\mathbf{s}'$. For the sake of clarity, we abstract this operation using a function F: $\{\text{set of all possible cell states}\} \rightarrow \{\text{set of all possible cell states}\}$, with $\mathbf{s}' = F(\mathbf{s}, x)$.

RNNs are prone to overfitting, hence not robust to errors in data collection. Further, they perform poorly when the dataset is highly varied and complex. Our model overcomes these issues by using the above-described state information $\mathbf{s}$ in a probabilistic setting to predict the next-step data. In other words, tDLGM uses latent relevant information from the past in order to predict the next data point. In particular, it predicts the parameters of the probability distribution of the next data point. There are other stochastic models for time-series data prediction, e.g., Time Generative Adversarial Network (Time-GAN) and Variational Recurrent Neural Network (VRNN) (Yoon et al., 2019; Chung et al., 2015).

1.1 Literature Survey

Previous nondeterministic models have been developed to address the issue of complex time-series data. Two notable examples are Time-GAN and VRNN (Yoon et al., 2019; Chung et al., 2015). Both models share a common characteristic, which is the idea of modeling a latent variable. We define ξ as a vector of latent variables and $\mathbf{v} \in \mathbf{V}$ as values from a time-series dataset. Both Time-GAN and VRNN base their design on Variational Auto-Encoder (VAE). It is used in situations where the prior of a latent variable is known $p(\xi)$, but the posterior $p(\xi \mid \mathbf{v})$ is not (Kingma, 2013). If the posterior is known then new data points can be accurately generated by sampling from the prior $p(\xi)$. VAE address this unknown relationship by approximating posteriors $p(\xi \mid \mathbf{v})$ through a recognition model. The approximated posteriors are then used to train a generator model. This generator model can then create new data points by sampling from the prior. VRNN and Time-GAN do this but with the additional constraint that their latent variables are conditioned on a state.

Time-GAN is based on the idea of a Generative Adversarial Network (GAN) (Yoon et al., 2019; Karras et al., 2017). The GAN architecture is usually constructed with one generator and one discriminator model. The generator is trained to create values, while the discriminator is trained to discern true and generated values. Time-GAN moves this to the latent space, meaning that the discriminator discerns between true and generated latent variables, and the generator is tasked with fooling the discriminator. The latent variables are parallel to this used to train another model, which reconstructs $\mathbf{v}$ from ξ.

VRNN has a more straightforward usage of inference (Chung et al., 2015). It trains a set of neural networks based on previous states that approximate a latent variables. Samples from this distribution are then used to generate values Our model has properties similar to VRNN. We will, therefore, discuss VRNN in further detail in the next section.

1.2 Our Contributions and Place in Literature

As previously stated, VRNN is based on the idea of VAE, which can be used when the prior of a latent variable is known ($p(\xi)$), but the posterior ($p(\xi \mid \mathbf{v})$) is not (Kingma, 2013). VRNN solves this by training a function that extracts latent variables from previous states. VRNN does this through two samples per time-step t. Specifically, given previous state $\mathbf{s}_{t-1}$ they define a latent variable as

$$\xi_t \sim \mathcal{N}(\mu_{0,t}, \sigma^2_{0,t}), \tag{1}$$

where $[\mu_{0,t}, \sigma_{0,t}] = p(\mathbf{s}_{t-1})$ and p is typically a neural network. This is then used to sample a value $\mathbf{v}$

$$\mathbf{v}_t \sim \mathcal{N}(\mu_{x,t}, \sigma^2_{x,t}), \tag{2}$$

where $[\mu_{x,t}, \sigma_{x,t}] = p_x(p_z(\xi_t), \mathbf{s}_{t-1})$ and, p_x and p_z are both neural networks. This structure, with one sample for the latent variable and another to generate $\mathbf{v}$ works well for time-series data. However, we believe that two layers of sampling hinder the potential robustness of the generative model. More samples can result in more intricate distributions. Therefore, we want a generative model for time-series data in which the layers of combined samples can be set as a parameter of the model.

Deep Latent Gaussian Model (DLGM) was developed by Rezende et al. in 2014 to solve the issue of scaleable inference in deep neural network model (Rezende et al., 2014). It is trained through approximate inference in layers and, as such, combines multiple Gaussian samples. This means that the number of layered samples can vary depending on the dataset's needs, allowing for more complex distributions compared to VRNN where there are two layers. This allows DLGM to learn complex patterns, generate new values, and perform inference. However, it cannot, despite these excellent properties, accommodate time-series data. We address this by combining DLGM with the idea of latent variables conditioned on states. The result is a novel recognition-generator structure that utilizes two recognition models, one for state and one for latent variables. It differs from VRNN through the use of two recognition models and the interleaving of state and latent variables.

To our knowledge, this model, called tDLGM, is new to literature. We believe this interleaving of state and latent variables structure should be as good, or better than, VRNN at learning temporal information from a dataset. The structure of sampling in layers should allow it to learn more complex distributions and be more robust against erroneous or faulty data. Our belief is based on the fact that a single-layered tDLGM reduces down to a structure similar to that of VRNN.

The two main contributions of this paper are:

- We introduce a novel model called tDLGM, which can learn complex temporal data. We show that this model is robust and performs well in a multitude of application areas.
- We introduce a novel recognition model called the state recognition model, based on the internal cell state of LSTM. We believe this application of the cell state is a novel contribution to the literature.

This paper is a continuation of the master thesis of Anton Johansson (Johansson, 2024). This paper further develops the work presented there, with an added improvements with respect to robustness and a more formal derivation of our loss function.

The rest of this paper is organized as follows. First comes a section that presents the main equations of DLGM and the modifications done to construct tDLGM. Following this is a series of derivations resulting in a well-defined generative model. Our third chapter presents the experiments, the results of which are discussed in chapter four. We then end with a conclusion chapter summarizing the paper and discussing future directions.

2 TIME-SERIES DEEP LATENT GAUSSIAN MODEL

DLGM is a generative model based upon the ideas of Gaussian mixture models (Rezende et al., 2014). It combines layers of Gaussian noise to generate complex distributions. It is trained through a recognition-generator structure. Where the recognition model is tasked with extracting the latent information from true values, which the generator model is trained to reconstruct.

DLGM's generator model can be defined through a series of equations

$$\xi_l \sim \mathcal{N}(\xi_l|\mathbf{0},\mathbf{I}), \quad l = 1, \ldots, L, \tag{3}$$

$$\mathbf{h}_L = \mathbf{G}_L \xi_L, \tag{4}$$

$$\mathbf{h}_l = T_l(\mathbf{h}_{l+1}) + \mathbf{G}_l \xi_l, \quad l = 1, \ldots, L-1, \tag{5}$$

$$\mathbf{v} \sim \pi(\mathbf{v}|T_0(\mathbf{h}_1)), \tag{6}$$

where ξ is the latent variables, $\mathbf{G}$ are trainable matrices, T are Multi-Layer Perceptrons (MLPs) and $\mathbf{v}$ are vectors of values. The goal is to train this generator model to be similar to the true distribution $p(\mathbf{v})$. As previously discussed, this is done by training the generator model on the approximated posterior of the latent variables $p(\xi\,|\,\mathbf{v})$. This generator and recognition model are then trained through the use of the negative log-likelihood. Readers interested in the more in-depth details of DLGM are referenced to (Rezende et al., 2014). Note the lack of any mention of state in the presentation of DLGM. This is because it is a stateless model, which we will now address.

tDLGM is an extension of DLGM to incorporate time-series data. The generator of tDLGM is obtained by replacing every MLPs in Equation (5) with RNNs. It also differentiates itself from DLGM by having two recognition models instead of one. The first is called the "latent recognition model" and is similar to DLGM's recognition model. The second one is called the "state recognition model" and is a latent representation of temporal relationships. The generator architecture is illustrated in Figure 1. Where the generator is structured in terms of layers denoted by H. Values created by the topmost layer (H_L) are passed to the one below. The following layer, denoted by H_{L-1}, generates a new value by utilizing a state variable, defined as $S_{L-1,t-1}$ and a sample from the Gaussian distribution $\mathcal{N}(\mathbf{0},\mathbf{I})$.

The mean of this Gaussian is the zero vector, while the covariance is the identity matrix. This process is repeated until the last layer, where the value $\mathbf{v}$ is extracted. Each layer (except for H_L) has an additional function called F, which is the state transition function. It updates the state value on every layer after generation.

The generator utilizes a RNN on each layer, associated with the "latent temporal states". We abstractize them into one single "state" where $\mathbf{s}_t$ denotes the t^{th} vector of relevant temporal information. The state can also be divided into its corresponding layers. We use the notation $\mathbf{s}_{l,t}$ to denote layer and order in the generation sequence. For example, $\mathbf{s}_{2,5}$ is the state at layer 2 at step 5. We define the t^{th} vector of stateless latent information as ξ_t. It is now possible to define the current state as dependent on all previous states.

$$p(\mathbf{s}_T) = p(\mathbf{s}_0) \prod_{t=1}^{T-1} \left[p(\mathbf{s}_t|\mathbf{s}_{1:t-1}, \xi_t) \right], \tag{7}$$

where $\mathbf{s}_{T-m:t-1} = [\mathbf{s}_{T-m}, \ \ldots \ \mathbf{s}_{t-1}]$ We assume that the importance of any one state decreases to an upper limit m beyond which past states and latent variables

have no impact. Hence,

$$p(\mathbf{s}_T) = \prod_{t=T-m}^{T-1} [p(\mathbf{s}_t \,|\, \mathbf{s}_{T-m:t-1}, \xi_{t-1})]. \tag{8}$$

Our definition of $\mathbf{s}_t$ and F allows a multitude of different RNNs to be used. We have chosen to use the cell state of LSTM as our state space $\mathbf{S}$. This means that our state recognition model has a non-traditional way of recognizing states. We give it a series of inputs, discard the output, and then use the internal temporal representation (cell state) for our generator model. The usual method would be to utilize the output of the RNN as the state values. Using the cell state instead of the LSTM outputs allows us to utilize the learned temporal information over long horizons. To the best of our knowledge, this method of using the cell state instead of the LSTM output is new to literature.

tDLGMs generator model can now be defined as

$$\xi_{l,t} \sim \mathcal{N}(\xi_l|\mathbf{0},\mathbf{I}), \quad l = 1\,,\ldots,\,L, \tag{9}$$

$$\mathbf{h}_{L,t} = \mathbf{G}_L \xi_{L,t}, \tag{10}$$

$$\mathbf{h}_{l,t} = R_l(\mathbf{h}_{l+1,t}, \mathbf{s}_{l,t}) + \mathbf{G}_l \xi_{l,t}, \quad l = 1,\,\ldots,\,L-1, \tag{11}$$

$$\mathbf{s}_{l,t+1} = F_l(\mathbf{h}_{l-1,t}, \mathbf{s}_{l,t}), \quad l = 1,\ldots,L-1, \tag{12}$$

$$\mathbf{v}_t \sim \pi(\mathbf{v}|T_0(\mathbf{h}_{1,t})), \tag{13}$$

where each of the layers $l = 1,\ldots,L-1$ has its own RNN defined as R_l, G_l is a trainable matrix on each layer, and F_l is the previously discussed state transition functions on each layer. ξ is the latent variables sampled from the Gaussian with zero vector as the mean and identity matrix as the covariance. Again, we use LSTM for our RNNs. The chosen RNN dictates the nature of the states and state transition function. The state on each layer, denoted by $\mathbf{s}_{l,t}$, is, therefore, a vector of cell states that allow for the capture of long-term temporal information.

We will now go through the whole generation process. The model starts with a sample $\xi_{l,t}$ from a Gaussian with the zero vector as mean and identity matrix as covariance. It is combined with the matrix $\mathbf{G}_L$, resulting in H_L. H_L is then used in the layer below as input to the RNN defined as $R_{L-1}(H_L, \mathbf{s}_{L-1,t})$. The sum of R_{L-1} and $G_{L-1}\xi_{L-1,t}$ becomes the output of that layer, denoted by h_{L-1}, which is used in the layer below h_{L-2}. This repeats to the last layer h_1, which is then used in Equation (13). The h from the layer above (h_{l+1}) is also combined with $\mathbf{s}_{l,t}$ to create the next state as seen in Equation (12). The layered latent variables provide robustness to the stateful model by interleaving states and latent variables.

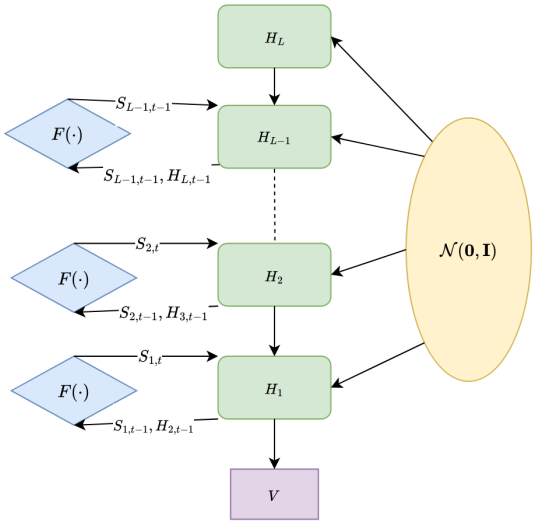

Figure 1: This figure shows how values are generated with tDLGM. It start at H_L which calculates its value by sampling from $\mathcal{N}(\mathbf{0},\mathbf{I})$. This result is then passed down to $\mathbf{H}_{l-1}$, which utilizes H_L, the current state, and a sample to calculate its value. This is done until the end, resulting in $\mathbf{v}$ as specified in Equation (13). It is also shown on the left-hand side how the state is updated by the function F on each layer.

Recall that VAE-based methods aim to approximate a posterior when a prior is fixed (Kingma, 2013). The same issue is present for tDLGM as we need to know both $p(\mathbf{s}\,|\,\mathbf{v})$ and $p(\xi\,|\,\mathbf{v})$. We have two recognition models for this, one being the state recognition model defined as k and another for the latent variable defined as q.

Starting with q, which can utilize a method similar to that of DLGM, see section 4.1 of (Rezende et al., 2014). That is, we define a posterior for the latent variable as

$$q(\xi\,|\,\mathbf{V}) = \prod_{t=1}^{T}\prod_{l=1}^{L} \mathcal{N}(\xi_{l,t}\,|\mu_l(\mathbf{v}_t), \mathbf{C}_l(\mathbf{v}_t)), \tag{14}$$

where the mean μ and covariance $\mathbf{C}$ on each layer are trainable. We take a more novel approach to the state recognition model. Recall Equation (12), which is responsible for creating future states that are, as defined by Equation (8), dependent on m previous states and latent variables. If the m previous states and latent variables were known, then it would be possible to train the state transition function F directly. However, since this is not known, we instead have to approximate the state on each layer

$$F_l(\mathbf{s}_{l,t}, \mathbf{h}_{l+1:L,t}) \approx \hat{F}_l(\mathbf{v}_{t-m:t}) = \mathbf{s}_{l,t} \tag{15}$$

where l is the corresponding layer, see Equation (12). Although we previously defined F_l as a function of $\mathbf{s}$ and $\mathbf{h}$ in Equation (12), F_l is also implicitly dependent

on ξ as $\mathbf{h}$ is dependent on it. Hence, with a slight abuse of notation, we say that

$$F_l(\mathbf{s}_{l,t}, \mathbf{h}_{l+1:L,t}) = F_l(\mathbf{s}_{l,t}, \xi_{l+1:L,t}), \tag{16}$$

making the relationship more explicit. It has the additional benefit of a cleaner-looking loss function without altering the underlying implementation.

We further define F and $\hat{F}$, where $F(\mathbf{s}_t, \xi_t) = [F_1(\mathbf{s}_{1,t}, \xi_{l+1:L,t}), \ldots, F_{L-1}(\mathbf{s}_{L-1,t}, \xi_{L,t})]$ and $\hat{F}(\mathbf{v}_{t-m:t}) = [\hat{F}_1(\mathbf{v}_{t-m:t}), \ldots, \hat{F}_{L-1}(\mathbf{v}_{t-m:t})]$ From this point forward, we no longer use the individual layer. Instead, we use our layer-agnostic definitions. We can then define the approximation as

$$k(\mathbf{S} \mid \mathbf{V}) = \prod_{t=1}^{T} (\mathbf{s}_{l,t} \mid \hat{F}(\mathbf{v}_{t-m:t-1})), \tag{17}$$

or stated another way

$$p(\mathbf{s}_t \mid \mathbf{s}_{t-m:t-1}, \xi_{t-m:t-1}) \approx k(\mathbf{s}_t \mid \mathbf{v}_{t-m:t-1}), \tag{18}$$

this solution is not yet complete. An issue arises due to the unknown prior $p(\mathbf{s})$. This means that the usual VAE method cannot be utilized. We will address this during the derivation of our loss function.

2.1 Deriving the Loss Function

We are now ready to derive the tDLGM loss function. Broadly speaking, the goal of tDLGM is to maximize the likelihood of generating the training data $\mathbf{V}$. Technically, it is achieved by minimizing the negative log-likelihood given by

$$\begin{aligned} \mathcal{L}(\mathbf{V}) &= -\log p(\mathbf{V}) \\ &= -\log \int_{\mathbf{S}} \int_{\xi} p(\mathbf{V}|\xi, \mathbf{S}) p(\xi, \mathbf{S}) d\xi d\mathbf{S}, \end{aligned} \tag{19}$$

The negative log-likelihood loss is an integral over $\mathbf{S} \times \xi$, which is the cross product of the state and latent variable space.

Both $\mathbf{s}$ and ξ have unknown posteriors $p(\mathbf{s}|\mathbf{v})$ and $p(\xi|\mathbf{v})$ which was addressed in the previous section by introducing two recognition models: the state recognition model $k(\mathbf{s}|\mathbf{v}) \approx p(\mathbf{s}|\mathbf{v})$ and the latent recognition model $q(\xi|\mathbf{v}) \approx p(\xi|\mathbf{v})$. We, for the sake of brevity, define $k(\mathbf{s})q(\xi) = \beta(\mathbf{s}, \xi)$. Both recognition models are included in the loss. Jensen's inequality is then used to get a surrogate loss

$$\begin{aligned} \mathcal{L}(\mathbf{V}) &= -\log \int_{\mathbf{S}} \int_{\xi} \frac{\beta(\mathbf{s}, \xi)}{\beta(\mathbf{s}, \xi)} p(\mathbf{V}|\xi, \mathbf{S}) p(\xi, \mathbf{S}) d\xi d\mathbf{S} \\ &\leq -\int_{\mathbf{S}} \int_{\xi} \beta(\mathbf{s}, \xi) \log \left(\frac{p(\mathbf{V}|\xi, \mathbf{S}) p(\xi, \mathbf{S})}{\beta(\mathbf{s}, \xi)} \right) d\xi d\mathbf{S}, \end{aligned} \tag{20}$$

the properties of the logarithm and the fact that the integral of a probability density function is equal to one leaves us with

$$\begin{aligned} \mathcal{L}(\mathbf{v}) \leq D_{KL}(k(\mathbf{S})||p(\mathbf{S})) + D_{KL}(q(\xi)||p(\xi)) - \\ \mathbb{E}_{q(\xi),k(\mathbf{S})}[log(p(\mathbf{V}|\mathbf{S}, \xi))]. \end{aligned} \tag{21}$$

Recall the definition of the posterior in Equation (14). We use this to say that

$$D_{KL}(q(\xi)||p(\xi)) = D_{KL}(\mathcal{N}(\mu, \mathbf{C})||\mathcal{N}(\mathbf{0}, \mathbf{1})). \tag{22}$$

which we will solve analytically.

The probability for k has been previously defined as

$$p(\mathbf{s}_t|\mathbf{s}_{t-m:t-1}, \xi_{t-m:t-1}) \approx k(\mathbf{s}_t|\mathbf{v}_{t-m:t-1}), \tag{23}$$

state, latent variables, and how they influence the current state is approximated based on true values $\mathbf{v}$. It is then possible to use an approximated state for the generation of future states

$$\begin{aligned} p(\mathbf{s}_{t+1} \mid F(\mathbf{s}_{t-m:t}, \xi_{t-m:t})) \approx \\ p(\mathbf{s}_{t+1} \mid F(\hat{F}(\mathbf{v}_{t-m:t-1}), \xi_t)), \end{aligned} \tag{24}$$

meaning that we use $\hat{F}$ to approximate an intermediate state $\mathbf{s}_t$. This intermediate state is then used by the generator model to generate the next state $\mathbf{s}_{t+1}$. This is useful as it allows us to generate an approximate state through two methods. The first method uses the approximation function $\hat{F}$. While the second method receives an approximation from $\hat{F}$, which is then used in the true state transition function F. Applying this to the KL divergence results in

$$\begin{aligned} D_{KL}(k(\mathbf{S})||p(\mathbf{S})) &= D_{KL}(k(\mathbf{S}_{t+1})||p(\mathbf{S}_{t+1})) \\ &\approx D_{KL}(k(\mathbf{S}_{t+1})||p(F(k(\mathbf{S}_t|\mathbf{V}_{t-m:t}), \xi_t)). \end{aligned} \tag{25}$$

Our final issue arises because it is difficult to calculate the above KL-divergence. This is the case because both F and $\hat{F}$ are deterministic functions, and the prior $p(\mathbf{s})$ is unknown. We addressed this by calculating the Mean Squared Error (MSE)

$$D_{KL}(k(\mathbf{S})||p(\mathbf{S})) \simeq \alpha \text{MSE}(\hat{F}(\mathbf{V}_{t+1}), F(\hat{F}(\mathbf{V}_t), \xi_t)), \tag{26}$$

where α is added as a scaling factor to account for the fact that the KL-divergence and MSE are different metrics. To summarize, we approximate $\mathbf{s}_t$ with function $\hat{F}(\mathbf{v}_{t-m:t-1}) = \mathbf{s}_t$. Our approximation is then used to generate $\mathbf{s}_{t+1}$, $F(\hat{F}(\mathbf{v}_{t-m:t-1}), \xi_t) = \mathbf{s}_{t+1}$. This generated state is then compared against an approximated state through $\text{MSE}(\hat{F}(\mathbf{v}_t), F(\hat{F}(\mathbf{v}_{t-1}, h_t)))$. Recall that we are comparing the cell state as created by the state recognition model and the generator model. Minimizing the MSE means that we train the state recognition model and generator model to

Another alternative is to predict the distribution of the next state with our state recognition model. The KL-divergence can then be approximated as a log-likelihood instead of MSE.

Equations (22) and (26) can then be applied in the surrogate loss

$$\begin{aligned}\mathcal{L}(\mathbf{V}) &\leq D_{KL}(k(\mathbf{S})||p(\mathbf{S})) + D_{KL}(q(\xi)||p(\xi)) \\ &\quad - \mathbb{E}_{q(\xi),k(\mathbf{S})}[\log(p(\mathbf{V}|\mathbf{s},\xi))] \\ &\approx D_{KL}(\mathcal{N}(\mu,\mathbf{C}))||\mathcal{N}(\mathbf{0},\mathbf{I})) \\ &\quad + \alpha\text{MSE}(F(\mathbf{V}_{t+1}), F(\hat{F}(\mathbf{V}_t), h(\xi_t) \\ &\quad - \mathbb{E}_{q(\xi),k(\mathbf{S})}[\log(p(\mathbf{V}|\mathbf{s},\xi))],\end{aligned} \tag{27}$$

where the KL-divergence can be calculated analytically, resulting in the final loss

$$\begin{aligned}&\frac{1}{2}\sum_{l,n}[||\mu_{n,l}||^2 + Tr(C_{n,l}) - \log|C_{n,l}| - 1] \\ &\qquad + \alpha\, MSE(k(\boldsymbol{S}^+), p(\boldsymbol{S}^+)) \\ &\qquad - \mathbb{E}_{q(\boldsymbol{\xi}),k(\boldsymbol{s})}[log((p(\boldsymbol{v}|\boldsymbol{s},\boldsymbol{\xi},\theta)p(\theta))].\end{aligned} \tag{28}$$

3 EXPERIMENTS [1]

Our experiments were performed with a dataset provided by Alibaba under a free license for research use (Weng et al., 2023). It is a tabular dataset containing traces of different data center tasks with their timestamps, resource requirements, etc. We are interested in the column associated with the GPU requirements - titled `GPU_MILLI`. Also note that the arrival, deletion, and schedule times are discarded. In other words, we are only interested in predicting the next GPU requirement not when it arrives.

tDLGM is compared to two baseline models. Our first baseline model is a traditional RNN consisting of LSTM units (Hochreiter and Schmidhuber, 1997). While DLGM is used as the second baseline model (Rezende et al., 2014). DLGM, as previously discussed, is stateless and therefore the vanilla version cannot be used for time-series prediction tDLGM. In order to still use it as a baseline, we provide as input a fixed length vector of historical data for the next-step prediction. Thereby explicitly providing temporal data relations within the history that is provided as input DLGM. With this modification, we still expect poor performance since the dataset has very long-term temporal connections between data points that will probably be missed by the provided historical vector. *It is worth noting that the historical vector is only provided as input during training and not during the data generation stage.*

[1]The code for tDLGM can be found here: https://git.cs.kau.se/johaanto/tdlgm

As mentioned in the Abstract and Introduction, we are interested in robust Generative AI models. Models such as RNN and DLGM are not known to be robust. Here, robustness is achieved by adding low variance Gaussian noise to the training data in the hope that this would simulate any real-world noise that is encountered during prediction (testing phase). For example, the authors of DLGM found that it could only reconstruct effectively when noise was artificially injected into the training dataset (Rezende et al., 2014). On the other hand, we train tDLGM on the given unaltered dataset. We test its efficacy with respect to both reconstruction and data generation using noisy test data. *In short, it beats the baselines.* Further, there was no statistically significant performance degradation due to the presence of noise in the testing phase that was absent during the training phase. Through this, we concluded that tDLGM is robust to additive Gaussian noise.

Generally speaking, a time-series predictor is either used for data imputation or for lookahead purposes (predict the future). A good predictor must predict reliably over longer time horizons. In recent years, robustness to data errors has also become a desirable property. Hence, we compare tDLGM to the baselines with respect to imputation performance, prediction error as a function of the prediction horizon, and with respect to robustness to data errors. Below, we describe them in further detail.

1. **Imputation,** where we feed noisy data (additive Gaussian noise) into our models and see how well they reconstruct the true data. The imputation is performed on test data that was not used during training. As the dataset is simple, and since we explicitly feed DLGM with temporal information, we expect it to perform well. We observed that DLGM has the lowest MSE capable of reconstructing close to perfectly, followed by tDLGM. However, we argue that the lower MSE and variance of DLGM do not mean it is better than tDLGM. This will be discussed in the Results section.

   RNN, on the other hand, has significantly worse performance, as illustrated in Figure 2. We repeated the experiments with varying levels of added Gaussian noise.

2. **Multiple time-step prediction,** where we require the models to predict over multiple time-steps in the future. This set of experiments is important since it is known that prediction errors typically accumulate over time when predicting over multiple steps. This is because predicted values are themselves used to predict more values that are further into the future. We may consider two met-

rics: the average mean squared error over the prediction horizon and the similarity of the generated values to the true distribution. We use the latter since we are interested in the model's ability to capture trends in the given time-series dataset. We are not interested in exactly duplicating the dataset. Standard metrics such as MSE score how well a generative model can predict given data points. One of our future goals is to use this generative model in cases where the data is limited. If it were to recreate the already limited dataset accurately, it would lose its purpose. We want it to generate new but similar data, not the same data. The used metric is explained in Algorithm 1. tDLGM performed best, followed by DLGM and then RNN.

3. **Robustness,** where we check by how much the model performances degrade due to errors in the dataset. One core idea of tDLGM is that interleaving state and latent variables should facilitate robust prediction. That is, the generative model should still be able to perform given uncertainties in data. One previously discussed method of increasing robustness is to train a model on noisy data. DLGM, for example, struggled with recognition of unseen data without this (Rezende et al., 2014). Therefore, we want tDLGM to reconstruct unseen data without training it on noisy data. Our tests prove that tDLGM can reconstruct without training on noisy data, validating the claim that tDLGM is robust.

As mentioned before, adding Gaussian noise to the training dataset is one way Machine Learning engineers hope to achieve robustness. In some cases, artificially injecting errors into the dataset can be a requirement for good learning (Rezende et al., 2014). However, what happens if we train for one kind of error but encounter errors of another type during testing? For example, mean zero low variance Gaussian noise is typically added to training data for this purpose. What if we encounter biased noise during testing? Hence, the artificial noise injected must be problem-specific. Learning models such as ours exhibit robustness properties and are better equipped to handle such problematic scenarios.

4 RESULTS

Since the data was not very complex (limited long-term temporal dependencies), and since we explicitly provided a vector of past history as input to DLGM, it performed well when it came to data reconstruction.

Data: $T \leftarrow$ true data
Data: $G \leftarrow$ generated data
Data: $s \leftarrow$ step forward in time
Data: $TM \leftarrow$ matrix initialized to zero
Data: $GM \leftarrow$ matrix initialized to zero
for $t_i \in T, \forall t_i, where\ t_{i+s} \in T$ **do**
  $TM_{t_i,t_{i+s}} \leftarrow TM_{t_i,t_{i+s}} + 1$
end
for $g_i \in G, \forall t_i, where\ g_{i+s} \in G$ **do**
  $GM_{g_i,g_{i+s}} \leftarrow GM_{g_i,g_{i+s}} + 1$
end
$GM \leftarrow {}^{|T|}/_{|G|} \times GM$ Scale values in GM based on amount of data points.
$score = \sum_i \sum_j {}^{\min(GM_{i,j},TM_{i,j})}/_{TM_{i,j}}, \forall i, j\ TM_{i,j} \neq 0$

Algorithm 1: Evaluation of future prediction. Models are scored by grouping their generated values into intervals. The algorithm then counts how many instances of a specific value are generated after another value. Therefore, distributions are formed over what values are usually generated when. The overlap between the true and generated distributions is then used as the score. It assumes that T and G contain a finite set of values corresponding to intervals, or so-called buckets of values. Scaling is also performed, accounting for the fact that T and G might have different amounts of values.

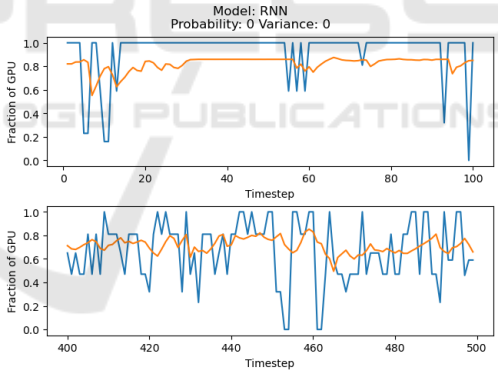

Figure 2: The best performing RNN model for reconstruction when using a naive MSE scoring method. Blue are the true values and orange is the generated values. The Y-axis specifies what fraction of a GPU a task at a specific step requires, with a maximum of 1 and minimum of 0. It is evident that the reconstruction process performs poorly.

With tDLGM as a close second, the basic RNN performed worst out of all the models. See Table 1 for a complete table of the different values that were tried and their mean squared error. Here, it is evident that DLGM was almost unaffected by the noise, generating accurate values with close to the same variance for all cases. RNN is also unaffected. This is because noise was added to the training data before training the DLGM and RNN models - a standard practice to

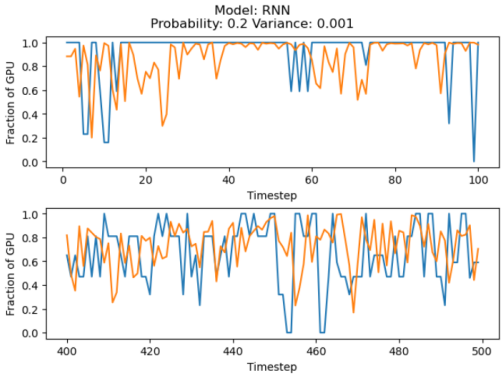

Figure 3: A model that performed worse than the best performing RNN when using a naive MSE scoring method. Blue represents true values, and orange represents the generated values. The Y-axis specifies what fraction of a GPU a task at a specific step requires, with a max of 1 and a minimum of 0. The probability and variance denote the introduction of error. With the probability denoting the likelihood of modifying a value and the variance specifying the magnitude of change according to a Gaussian.

improve the robustness of models that are not inherently robust. Figure 2 shows a slice of the best reconstruction, while figure 3 shows the worst slice (according to the mean squared error metric). From a visual inspection, it appears that the *worser* model follows the pattern while the better scoring model does not. Therefore, a filtering process is performed in the form of a t-test. It looks at the changes in the reconstructed data given different levels of additive noise. This filtering assumes that the reconstruction is negatively affected to such a degree that it is statistically significant. All trained instances with a p-value above 0.7 were excluded, leaving us with the new values we call Filtered RNN in Table 1. The high p-value is set to counteract the risk of confirmation bias. We assume that the error increases with the noise but do not want to filter out evidence proving the contrary.

Our new results make it evident that RNN is much more sensitive to noise as compared to both tDLGM and DLGM. Hence, we conclude that tDLGM performs better than the regular RNN at value imputation. Figures 7, 8, and 9 show the reconstruction without any noise for tDLGM, DLGM, and RNN respectively. Reconstruction with noise can be seen in Figures 4, 6, and 5. DLGM's ability to perfectly reconstruct should not be interpreted as it being a better model as compared to tDLGM. The simplicity of the data means that DLGM can easily overfit. Besides, perfect reconstruction is an indication that the model does not generalize well. It is better to have a reconstruction model - such as tDLGM - that generates similar values, but not exact values. This is also an indication of the robustness of tDLGM. Further research must be conducted with higher dimensional and more complex time-series data, to see how this changes performance.

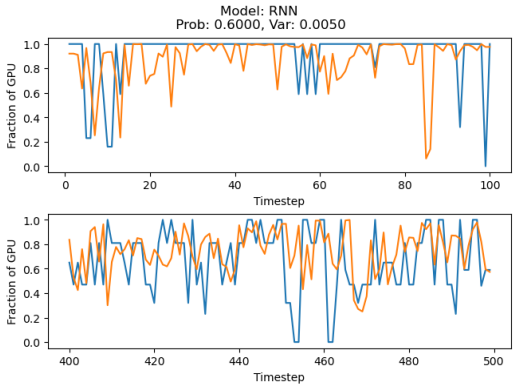

(a) Probability of modifying value: 60%, modifying through a Gaussian with variance set to 0.005.

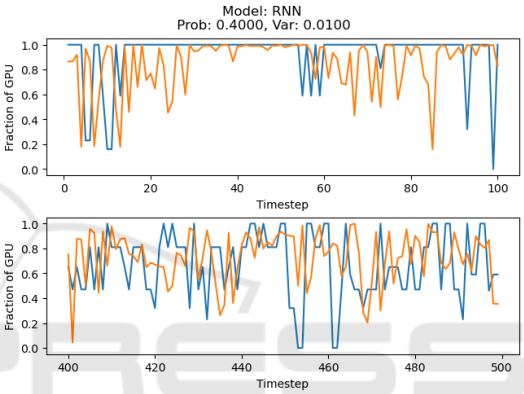

(b) Probability of modifying value: 40%, modifying through a Gaussian with variance set to 0.01.

Figure 4: RNN tasked with reconstructing the test dataset. The orange line is generated values, and the blue is true values. The X-axis is time. The Y-axis specifies what fraction of a GPU a task requires at a specific step, with a maximum of 1 and a minimum of 0.

In order to evaluate the data generation capability, we score based on the multiple-time-step prediction distributions - check if they match the empirical future distributions estimated from the dataset. We do not compare the values themselves, e.g., using mean-squared error. We are interested in the distribution of future values not the actual values themselves. Algorithm 1 describes this metric. Scoring is done on a dataset of future generations. It was generated by giving each model a sequence of values, which was then used to create future values see Table 2 for results. RNN performs well for shorter prediction horizons. However, it quickly deteriorates when generating longer sequences. tDLGM is stable with close to the same score no matter how long the prediction

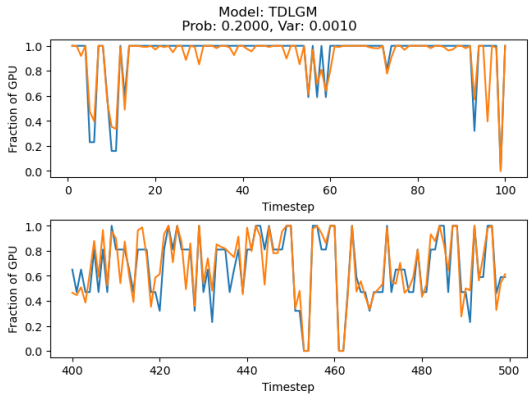

(a) Probability of modifying value: 20%, modifying through a Gaussian with variance set to 0.001.

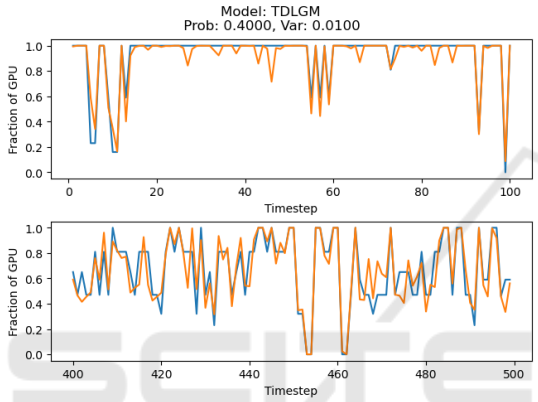

(b) Probability of modifying value: 40%, modifying through a Gaussian with variance set to 0.01.

Figure 5: tDLGM tasked with reconstructing the test dataset. The orange line is generated values, and the blue is true values. The X-axis is time. The Y-axis specifies what fraction of a GPU a task requires at a specific step, with a maximum of 1 and a minimum of 0. Subfigures 5a and 5b show the model's performance with different noise levels added.

horizon is set to. DLGM also exhibit this stable behavior but with a lower score than tDLGM. From this, we conclude that tDLGM provides a more consistent data generation as compared to RNN and DLGM.

We will now discuss the robustness of tDLGM. Models are usually trained by combining true values with artificial noise, a common practice to improve robustness. If tDLGM exhibits robustness properties, then this should not be required. We evaluated this by training tDLGM with the unmodified training data and then performed reconstructions (imputation). Reconstructions were, as before, performed with varying magnitudes of noise. Our results can be seen in Table 3. Here, it is evident that the reconstruction performed more or less similarly without the added noise. Although it was still significantly better than that of RNN, which can be seen in Table 1. We conclude

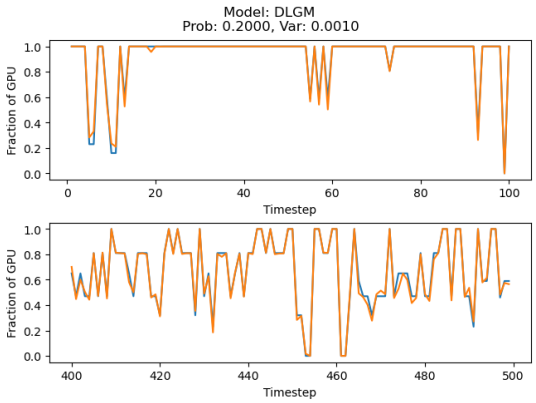

(a) Probability of modifying value: 20%, modifying through a Gaussian with variance set to 0.001.

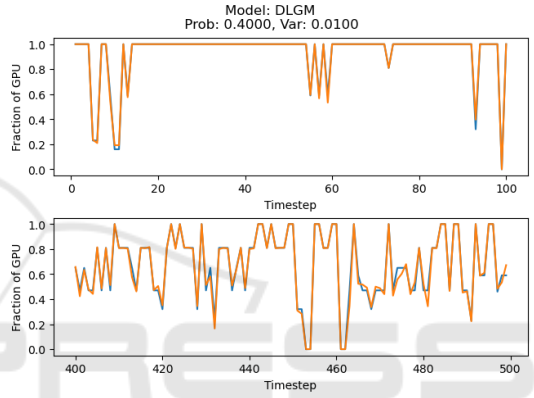

(b) Probability of modifying value: 40%, modifying through a Gaussian with variance set to 0.01.

Figure 6: DLGM tasked with reconstructing the test dataset. The orange line is generated values, and the blue is true values. The X-axis is time. The Y-axis specifies what fraction of a GPU a task requires at a specific step, with a maximum of 1 and a minimum of 0. Subfigures 6a and 6b show the model's performance with different noise levels added.

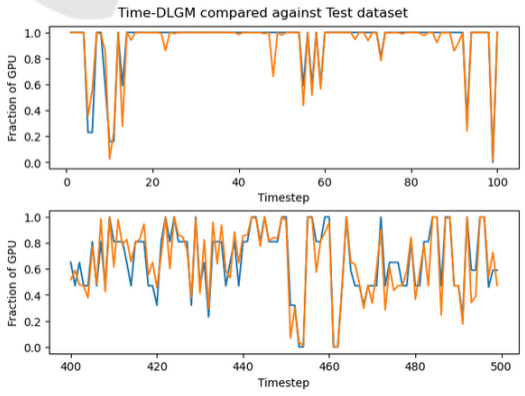

Figure 7: tDLGM tasked with reconstructing the test dataset. Orange is generated values and blue is true values. The X-axis is time. The Y-axis specifies what fraction of a GPU a task at a specific step requires with a max of 1 and 0 as minimum. It is evident from the figure that tDLGM can reconstruct the data.

Table 1: Table showing how well the different models reconstructed the test data. Each data point had a percentual chance of being modified through a Gaussian sample. The variance was modified to see how each model reacted to different magnitudes of error.

Probability: 0, Variance: 0		
Model	MSE	Variance
tDLGM	0.0122	0.0083
DLGM	0.0006	7.0×10^{-6}
RNN	0.0773	0.0164
Filtered RNN	0.1038	0.0329
Probability: 0.2, Variance: 0.001		
Model	MSE	Variance
tDLGM	0.0122	0.0009
DLGM	0.0006	4.9×10^{-6}
RNN	0.0773	0.0164
Filtered RNN	0.0794	0.0153
Probability: 0.6, Variance: 0.005		
Model	MSE	Variance
tDLGM	0.0118	0.0124
DLGM	0.0006	4.8×10^{-6}
RNN	0.0773	0.0164
Filtered RNN	0.1033	0.0323
Probability: 0.4, Variance: 0.01		
Model	MSE	Variance
tDLGM	0.0114	0.0014
DLGM	0.0006	4.4×10^{-6}
RNN	0.0773	0.0164
Filtered RNN	0.0827	0.0172
Probability: 0.8, Variance: 0.05		
Model	MSE	Variance
tDLGM	0.0118	0.0008
DLGM	0.0007	6.8×10^{-6}
RNN	0.0773	0.0164
Filtered RNN	0.0788	0.0153

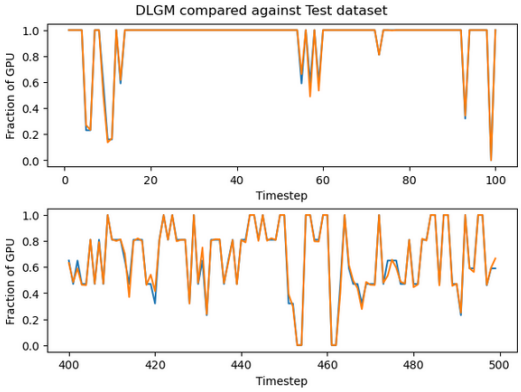

Figure 8: DLGM compared against the test dataset. Orange is the generated values, and blue is the true values. The X-axis is the steps in an unspecified time unit, where one generation is performed each step. The Y-axis specifies what fraction of a GPU a task at a specific step requires with a max of 1 and 0 as minimum. DLGM can perfectly reconstruct values in many instances, as evident by the high overlap.

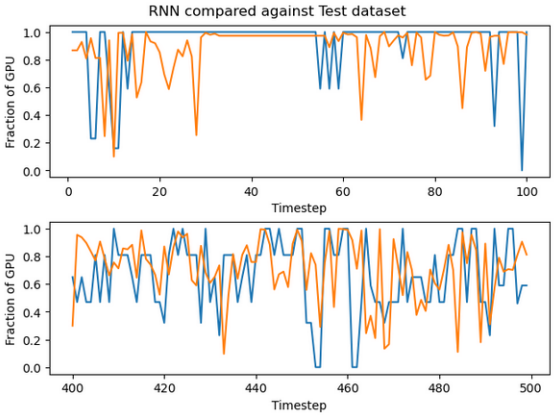

Figure 9: RNN tasked with reconstructing the test dataset. Orange is generated values and blue is true values. The X-axis is time. The Y-axis specifies what fraction of a GPU a task at a specific step requires with a max of 1 and 0 as minimum. It is evident from the figure that RNN can reconstruct data, although much worse than the other two models.

Table 2: Table showing how well the different models generated future values. A higher score correlates with a larger overlap between the true and generated values. Scoring is done with Algorithm 1. *Steps* defines the number of consecutive digits generated for each test. For example, a sequence length of 30 means that a state was fed, which was then used to create the following 30 values. We can conclude from this that tDLGM was best at generating future values that look similar to the actual distribution, followed by DLGM and then RNN.

Steps	tDLGM	RNN	DLGM
2	62.47	58.48	59.87
5	63.47	58.48	59.67
8	63.21	58.41	60.32
10	63.59	58.04	59.67
15	63.67	57.79	60.11
20	63.54	58.01	60.36
25	63.31	57.80	59.89
30	63.31	58.01	60.33

based on this that tDLGM is inherently robust and can generalize better to values outside of the training set without the need for any standard robustness-inducing techniques. Figures 10 show the reconstruction for two types of additive noise.

5 CONCLUSION

We have proposed a new model called tDLGM, based on the ideas of a recognition-generator structure with state. tDLGM differ from other models commonly seen in the literature by using two recognition models, one for state and one for latent variables. Both state and latent variables are combined in an interleaving

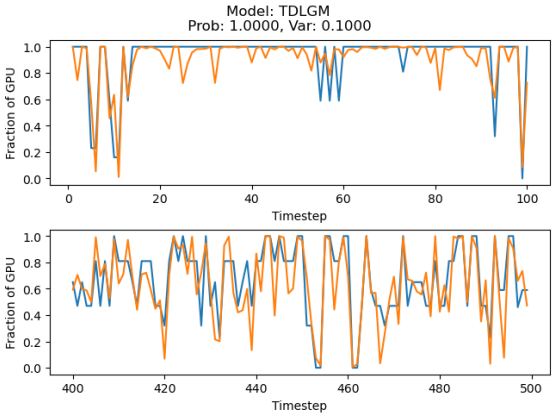

(a) Probability of modifying value: 100%, modifying through a Gaussian with variance set to 0.1.

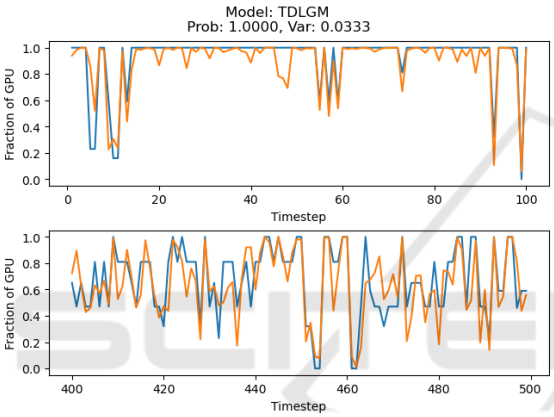

(b) Probability of modifying value: 100%, modifying through a Gaussian with variance set to 0.0333.

Figure 10: tDLGM tasked with reconstructing the test dataset. The orange line is generated values, and the blue is true values. The X-axis is time. The Y-axis specifies what fraction of a GPU a task requires at a specific step, with a maximum of 1 and a minimum of 0. Subfigures 10a and 10b show the model's performance with different noise levels added

structure, which allows for the learning of complex temporal relations. Furthermore, to our knowledge, the state recognition model and the regularization we derive from it are a novel inference method. Our experiments on the Alibaba trace dataset (Weng et al., 2023) show that tDLGM is a promising model with good performance with regard to imputation, the generation of new values, and robustness. We, through this, showed that tDLGM is a generative model suitable for modeling long-term temporal relationships.

However, there are also some points for future improvements. Due to the inherent complexity of tDLGM, we expect that it requires more data to train when compared to DLGM, which has a simpler architecture. Additionally, we did not spend an inordinate

Table 3: Table showing how well tDLGM managed to reconstruct unseen values based on different amounts of noise. Each data point in the test dataset was modified according to the Gaussian $\mathcal{N}(0,\sigma^2)$ where σ^2 is varied variance. The output was clamped to the range $[0,1]$. tDLGM was trained purely on the unmodified training data.

σ^2	MSE	Variance
0.0053	0.01306	0.00090
0.0059	0.01371	0.00099
0.0067	0.01214	0.00080
0.0077	0.01221	0.00079
0.0091	0.01275	0.00088
0.0111	0.01288	0.00086
0.0143	0.01287	0.00089
0.0200	0.01328	0.00095
0.0333	0.01315	0.00081
0.100	0.01938	0.00168

amount of time on hyperparameter optimization, instead opting for a simple grid search method. This was done because the ease of implementation was one of our goals. Hence, we experienced that training runs needed to be restarted with a probability of .25. We conjecture that this is due to the aforementioned complexity, the smaller dataset, and the need to extract temporal information. For more complex problems, we expect that more thorough hyperparameter optimization will be required in addition to a larger dataset.

Another avenue of future research is to make a more exhaustive comparison against other models for time-series data, such as VRNN (Chung et al., 2015). It would also be interesting to explore the approximation from Equation (26) in further detail.

REFERENCES

Chung, J., Gulcehre, C., Cho, K., and Bengio, Y. (2014). Empirical evaluation of gated recurrent neural networks on sequence modeling.

Chung, J., Kastner, K., Dinh, L., Goel, K., Courville, A. C., and Bengio, Y. (2015). A recurrent latent variable model for sequential data. *CoRR*, abs/1506.02216.

Hochreiter, S. and Schmidhuber, J. (1997). Long Short-Term Memory. *Neural Computation*, 9(8):1735–1780.

Johansson, A. (2024). Generative ai for time dependent data. Master's thesis, Karlstad University, Department of Mathematics and Computer Science (from 2013).

Karras, T., Aila, T., Laine, S., and Lehtinen, J. (2017). Progressive growing of gans for improved quality, stability, and variation. *arXiv preprint arXiv:1710.10196*.

Kingma, D. P. (2013). Auto-encoding variational bayes. *arXiv preprint arXiv:1312.6114*.

Mehmeti, F. and Porta, T. F. L. (2021). Analyzing a 5g dataset and modeling metrics of interest. In *2021*

17th International Conference on Mobility, Sensing and Networking (MSN), pages 81–88.

Rezende, D. J., Mohamed, S., and Wierstra, D. (2014). Stochastic backpropagation and approximate inference in deep generative models. In *International conference on machine learning*, pages 1278–1286. PMLR.

Weng, Q., Yang, L., Yu, Y., Wang, W., Tang, X., Yang, G., and Zhang, L. (2023). Beware of fragmentation: Scheduling gpu-sharing workloads with fragmentation gradient descent. In *2023 USENIX Annual Technical Conference*, USENIX ATC '23. USENIX Association.

Yin, H. and Berger, C. (2017). When to use what data set for your self-driving car algorithm: An overview of publicly available driving datasets. In *2017 IEEE 20th International Conference on Intelligent Transportation Systems (ITSC)*, pages 1–8.

Yoon, J., Jarrett, D., and Van der Schaar, M. (2019). Time-series generative adversarial networks. *Advances in neural information processing systems*, 32.